

The Small-Scale Variability of Electrical Soil Properties – Influence on GPR Measurements

Jan Igel
Leibniz Institute for Applied Geosciences
Hannover, Germany
email jan.igel@gga-hannover.de

Abstract – The spatial variability of electrical conductivity and permittivity of sandy soils is measured in situ and statistically analysed. Conductivity is determined with high resolution geoelectrical dipole-dipole measurements. Permittivity is determined with two GPR techniques: i) the coefficient of reflection is measured at the soil surface, ii) a new groundwave technique using two receiving antennas is presented which provides high spatial resolution. Variability of both electrical properties show to be high in sandy soils and feature correlation lengths of a few decimetres. Conductivity is log-normal distributed while permittivity is normal distributed. The statistical properties are used to generate synthetic random models which represent the soils in situ. These media are used for realistic FD calculations. The influence of soil heterogeneity is discussed by way of example for the problem of landmine detection with GPR. Variations of permittivity show to have greater influence on GPR measurements than variations of conductivity.

Keywords – conductivity, permittivity, soil properties, groundwave, spatial variability, geostatistics, FD simulation, landmine detection.

I. INTRODUCTION

Physical soil properties feature high variability in space and time which are known to affect geophysical measurements. The question to what extend soil heterogeneities influence near-surface GPR measurements is analysed by the following procedure:

- determining electrical soil properties in situ
- geostatistical analysis of the spatial variability of soil properties
- fitting a statistical model to the data
- geostatistical simulation to generate synthetic random media
- finite-differences (FD) calculation of electromagnetic wave propagation

Electromagnetic wave propagation is mainly influenced by dielectric permittivity and electric conductivity. The waves are reflected and scattered at soil heterogeneities to some extend. This is particularly the case if heterogeneities occur in the range of the wavelength of the radar signal which is typically in the order of 1 dm and some few metres for standard GPR applications.

Electrical soil properties are determined by various parameters as e.g. texture, bulk density, organic content, salinity and soil moisture. The latter is the most significant factor in the vadose zone and features high spatial variability which may be caused by water repellency, micro topography, soil aggregation and vegetation. Figure 1 shows a picture of a sandy soil whereas the turf has been removed. The pattern accords to the spatial moisture distribution and one can recognise high variability in the range of decimetres. This variability is typical for the topsoil which is the most heterogeneous soil part and occurs in horizontal and vertical direction.



Figure 1. Picture of sandy soil (1 m × 1 m) demonstrating soil heterogeneity: dark parts = moist soil, light parts = dry soil, (pers. comm. Schmalholz, TU Berlin, <www.interurban.de>).

To determine the electric soil properties in situ with the required high spatial resolution of decimetres, geophysical techniques had to be methodically enhanced.

II. ELECTRIC CONDUCTIVITY

Electric conductivity and its variability in the topsoil are determined with high resolution DC resistivity measurements. To get a high spatial resolution, a 2D and 3D dipole-dipole configurations are used with an electrode spacing of 0.1 m. With these setups variabilities in the range of decimetres can well be mapped inside the first 0.25 m of the soil [8]. As sandy soils are analysed and ionic conduction in the pore fluid is the dominant process of charge transport, the frequency dependence of conductivity is

small and the DC conductivities are used as HF (high frequency) approximation for the frequency range of GPR. This procedure might not be adequate when analysing other soils, e.g. possessing high clay contents which often feature significant frequency dependence of conductivity. In that case, the variabilities of the DC values have to be transformed into HF values.

III. DIELECTRIC PERMITTIVITY

Dielectric permittivity is determined by using 2 GPR methods basing on independent physical mechanisms. The groundwave technique uses the dependence of propagation velocity from soil permittivity and the reflection technique the dependence of the coefficient of reflection from the electrical properties at the soil surface.

3.1 Groundwave

The groundwave technique has been used to determine soil moisture for about 10 years [3, 6, 12, 13]. The groundwave is a plane wave travelling in the soil along the interface soil-air. Its appearance can be explained by over-critical refraction of spherical waves which are emitted by the transmitting antenna. It is the only wave travelling through the ground with a propagation path that is a priori known. Groundwave measurements have proven to be a fast technique which can be used to map large areas and yields reasonable results when compared to other methods like TDR or gravimetric soil moisture determination [7]. There are two modes the groundwave measurement can be carried out.

- A moveout (MO) or a common mid point (CMP) measurement is performed by separating the antennas. On a homogeneous halfspace, the groundwave onset appears as a straight line and its slope corresponds to the inverse of the propagation velocity in the soil.
- A constant offset (CO) measurement is carried out by moving the fixed transmitter-receiver layout along a profile and measuring lateral variations of the groundwave velocity. This is a fast technique to map large areas. However, it can be a challenge to identify the groundwave in solely a CO measurement especially in heterogeneous soils where many different phases may interfere.

A combination of both methods was proposed by Du [3] and showed to be the most appropriate approach to this date. First, a MO measurement is carried out to determine the groundwave velocity and the optimal distance between transmitter and receiver at which the groundwave does not interfere to neither the airwave nor reflected waves. Then, the setup is fixed and the profile is mapped by using a CO setup as illustrated in Figure 2.

This procedure has some basic disadvantages as it is time consuming and there may arise difficulties to determine proper ground wave velocity if soil is heterogeneous. One eminent disadvantage is the limited lateral resolution of the

method. It is determined by the minimal offset of transmitter and receiver at which air and ground wave are well separated in the radargram. The resolution is in between half and a few metres depending on the used antennas and the permittivity of the soil.

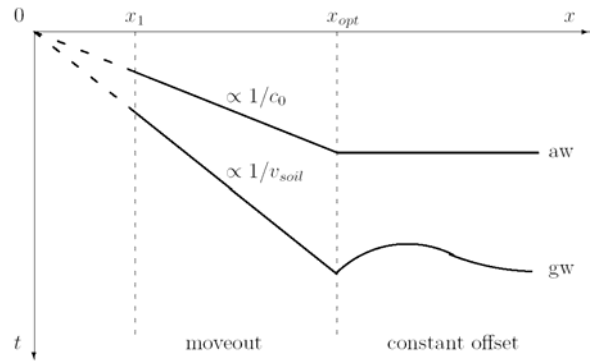


Figure 2. Schematic traveltime diagram of ground wave measurement consisting of a MO and from x_1 to the optimal distance x_{opt} followed by a CO measurement at $x > x_{opt}$. (aw: air wave, gw: groundwave).

To overcome these disadvantages, the groundwave measuring technique has to be methodically enhanced. The essential difference compared to the classical groundwave measuring technique as described above is to use two receiving antennas (Figure 3). Thus, only traveltime differences between the two channels have to be determined. The lateral resolution is not restricted by the minimal distance between transmitter and receiver any more but is determined by the distance between both receiving antennas. This distance is arbitrary and only limited by the dimensions of the antenna housings wherefore a high resolution can be achieved. As only traveltime differences between both receivers have to be determined, the onset of the air wave which is commonly used for time-zero calibration is not needed any more. Thus, shielded antennas can be used and the first onset detected at the receivers is the groundwave as neither the air wave nor critically refracted waves will be recorded. The only calibration which is needed is the synchronisation of both receiving channels at the beginning of the measurement to ensure that they rely on the same time basis, e.g. to account for different cable length.

Figure 3 shows a picture of the used setup. A shielded 500 MHz GSSI antenna is used as transmitter and two shielded 400 MHz antennas function as the receivers. The slightly different nominal antenna frequencies of transmitter and receivers will, if at all, affect both receiving channels in the same way. The distance between both receiving antennas is 0.14 m and the transmitter is separated 0.35 m of the first receiver.

The new layout has been experimentally tested in a sandbox. The sand was totally dry ($\epsilon_r = 3$) and an anomaly consisting of wet sand ($\Theta_v \approx 10$ vol%, $\epsilon_r = 5.8$) which was packed in a plastic foil was buried flush with the sandbox

top surface. A GPR measurement with the new setup described above was carried out along a transect over the anomaly. The groundwave traveltime differences Δt between both receivers are determined which allows the calculation of permittivity of the ground

$$\epsilon_r = \frac{c_0^2}{v^2} = \frac{c_0^2 \Delta t^2}{\Delta x^2},$$

where v is the groundwave velocity and Δx the separation of both receivers. The determined permittivities and the underground model, i.e. the permittivities determined with TDR (time domain reflectometry) fit quite well (Figure 4).

To demonstrate the lateral resolution of the 2-receiver technique, a FD (finite differences) calculation was performed [10]. The model consists of two anomalies ($\epsilon_r = 9$) of 10 cm width which are separated by 10 cm. They are embedded in a homogeneous medium with $\epsilon_r = 3$. A radar measurement was simulated using the layout described above. The groundwave onsets were picked and the traveltime was determined and transformed in permittivity values of the ground. The models and results are depicted in Figure 5. The black line corresponds to a classical groundwave measurement with only one receiving antenna and a transmitter-receiver distance of 0.7 m which is a realistic distance for field applications. One can recognise that both anomalies cannot be resolved and only one wide anomaly appears with a lower permittivity than in the model. In contrast, when using the 2-receiver setup (14 cm distance of both receivers) both anomalies can clearly be recognised and the deduced permittivity values fit quite well to the model.



Figure 3. Setup used for the groundwave measurements. A shielded bistatic 500 MHz GSSI antenna is used as transmitter and two bistatic 400 MHz GSSI antennas are the receivers. The position of the antennas in the housings are indicated whereas the active elements are in boldface (T = transmitter, R1 and R2 = receivers).

3.2 Coefficient of Reflection

The second method to determine soil permittivity is to measure the coefficient of reflection ρ of radar waves at the soil surface. It depends on magnetic permeability, electric conductivity and permittivity of the ground. For the range

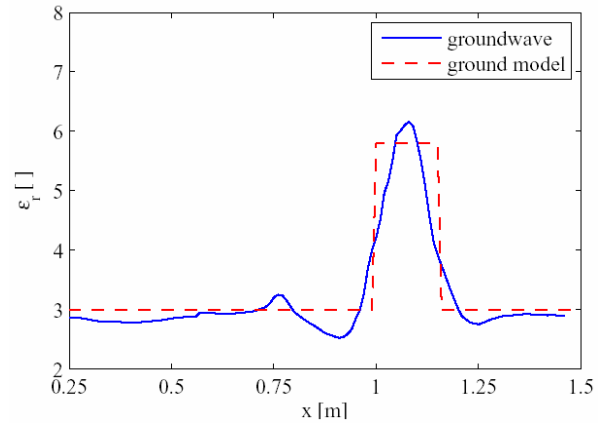


Figure 4. Groundwave experiment using the 2-receiver setup. A 0.15 m large anomaly of wet sand ($\epsilon_r = 5.8$) is placed in dry sand ($\epsilon_r = 3$). The result of the groundwave analysis is plotted as well as the ground model (ϵ_r values determined with TDR).

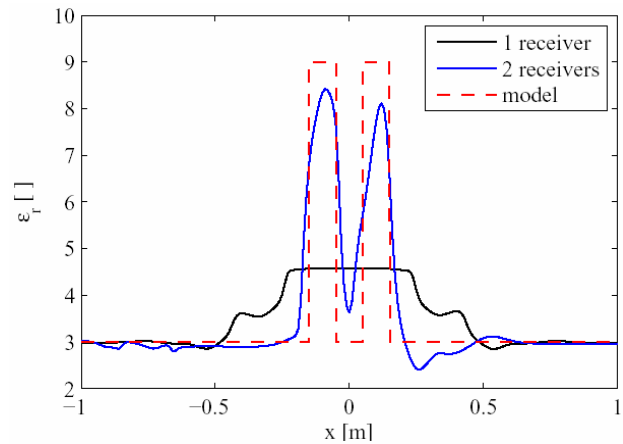


Figure 5. Results of FD groundwave analysis. The model is depicted in red, and the permittivity distribution determined from the simulated GPR measurement with two receiving antennas in blue. The result of a classical groundwave interpretation (0.7 m antenna offset) is plotted in black.

of properties which are typical for natural soils, only permittivity significantly affects the coefficient of reflection and permeability and conductivity can be neglected [8]. Thus, soil permittivity can be approximated by:

$$\epsilon_r = \left(\frac{1 - \rho}{1 + \rho} \right)^2.$$

In a strict sense, this equation holds only true for smooth surfaces. Soil roughness will change the coefficient of reflection but the differences are small if variations in topography are smaller than 1/10 of the wavelength [9]. The surfaces at the locations where the measurements are carried out can be regarded as smooth.

The field measurement is carried out by using a 1 GHz GSSI horn antenna which is mounted on a sledge to be operated at a distance of 0.5 m to the soil (Figure 6). At this distance, the direct wave inside the antenna and the reflected wave from the soil surface do not interfere any more. The horizontal resolution was experimentally determined to approximately 0.25 m [8].



Figure 6. Measuring setup to determine the coefficient of reflection: A 1 GHz GSSI horn antenna is mounted on a sledge 0.5 m above the ground.

IV. FIELD MEASUREMENTS AND STATISTICAL ANALYSIS

All field measurements were carried out on sandy soils which are used as grassland.

4.1 Conductivity

Figure 7 shows the resistivity (inverse of conductivity) distribution at a depth of 0.1 m as a result of a 3D dipole-dipole measurement (longitudinal and equatorial) on an area of 1.5 m \times 1.5 m after inversion [5]. One can recognize high spatial variability mainly caused by inhomogeneous moisture pattern as illustrated in Figure 1. Figure 8 shows the conductivity distribution along a 15 m long 2D profile. The ground is distinctly layered: heterogeneous topsoil overlays homogeneous subsoil. The interface between both soils at a depth of 0.25 m corresponds to the former ploughing horizon. Topsoil heterogeneity is probably caused by vegetation and root distribution and the resulting irregular water demand.

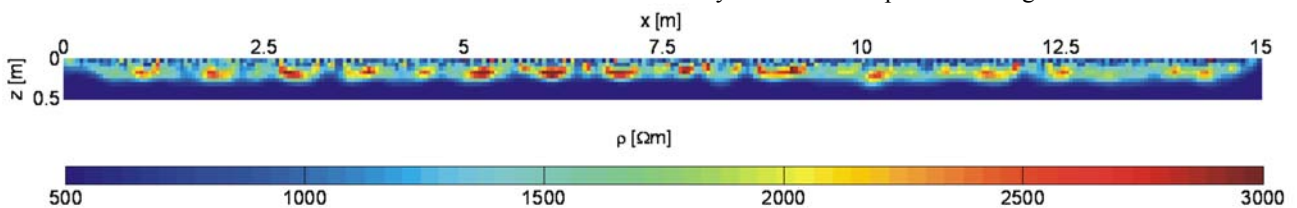


Figure 8. Resistivity distribution in a sandy soil along a 15 m long profile (inverted 2D dipole-dipole measurement).

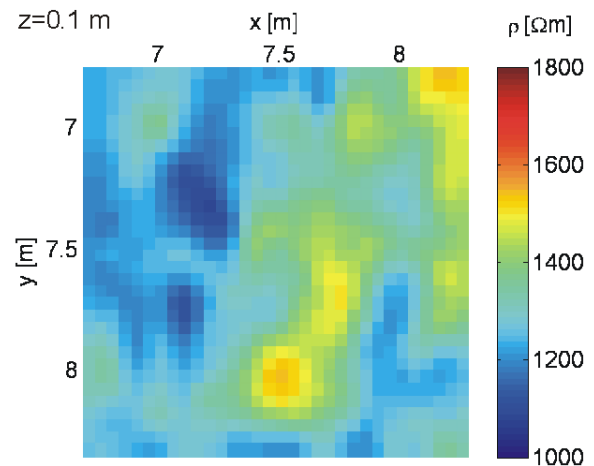


Figure 7. Resistivity distribution in the topsoil determined by 3D dipole-dipole resistivity measurements: horizontal cut at 0.1 m depth after inversion.

The conductivity of the topsoil is statistically analysed, i.e. the probability density function as well as the variogram is calculated for the first 0.25 m of the inverted models and a statistical model is fitted to the data (Figure 9). Conductivity is log-normally distributed with $\lg(\sigma/(S/m)) = -3.2 \pm 0.16$. An exponential variogram model was fitted with a correlation length of $a = 0.35$ m.

4.2 Permittivity

Permittivity distribution was determined on an area of 10 m \times 10 m on a regular grid. Before carrying out the GPR measurements, the grass was cut flush to the soil surface. Thus, the coefficient of reflection is not influenced by vegetation and a proper coupling of the antennas to the ground is ensured for the groundwave measurements.

Figure 10 shows the measuring grid for the GPR reflection measurement and the deduced permittivities for the profiles in y-direction. Permittivity distribution shows a stripe pattern in direction of approx. 30° with regard to the x-axis. Soil permittivity was determined on the same grid using the groundwave technique so that both methods can be compared. The probability density functions are plotted in Figure 11. In contrast to conductivity, permittivity is almost normal distributed (coefficient of reflection: $\epsilon_r = 4.6 \pm 0.9$, groundwave: $\epsilon_r = 5.3 \pm 0.85$). Due to the stripe pattern which can be seen in Figure 10, variogram analysis was performed in different directions. The semivariograms in x- and y-direction are plotted in Figure 12. The correlation

length in x-direction is much longer than in y-direction. An anisotropic variogram model was fitted with maximal correlation length a_{\max} being measured parallel to the stripes and shortest correlation length a_{\min} in the perpendicular direction whereby the anisotropy factor is $a_{\max}/a_{\min} = 5$.

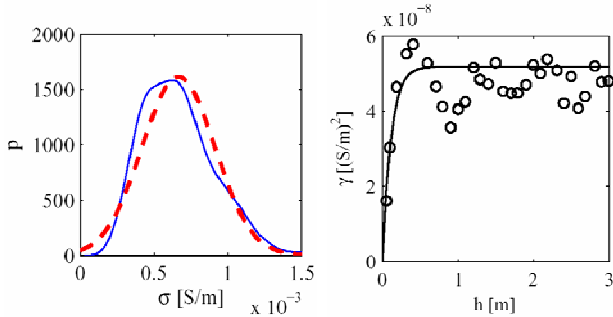


Figure 9. Conductivity distribution in the topsoil (first 25 cm): probability density function (left) and variogram analysis (right). Experimental data (blue line and circles), normal distribution (red dashed line) and exponential variogram model (black line).

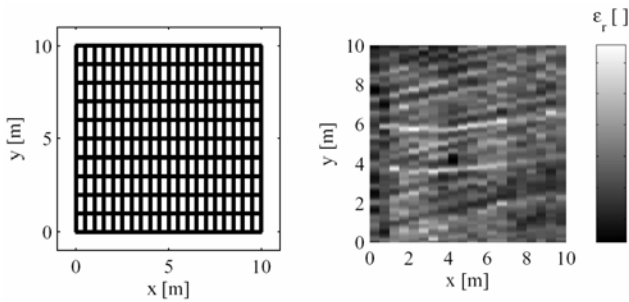


Figure 10. Measuring grid (left) and deduced permittivities from the coefficient of reflection of the profiles in v-direction (right).

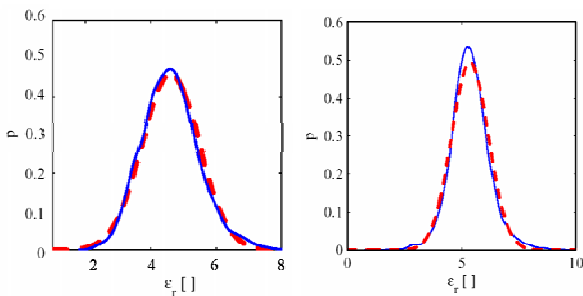


Figure 11. Probability density function of permittivity distribution. Experimental data (blue) and fitted normal distribution (red). Permittivity determined by the coefficient of reflection (left) and groundwave measurement (right).

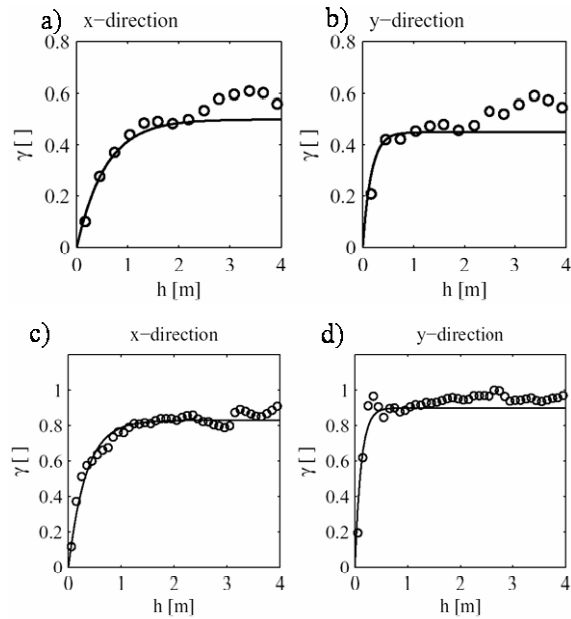


Figure 12. Variogram analysis of permittivity distribution. Experimental semivariance (circles) and fitted exponential variogram model (line). Permittivity determined by the coefficient of reflection (a,b) and groundwave measurement (c,d).

The determined parameters of the anisotropic variogram model are used for kriging the data. The results for the permittivities determined by both GPR methods are depicted in Figure 13. The periodical structure and the resulting anisotropy are probably caused by the former cultivation of the area. Until 2 years before the measurement were carried out on the grassland, the area had been used as an acre and the direction of the regular pattern (30°) corresponds to the former direction of cultivation. The periodical structure might be a relict of ploughing e.g. due to compaction of the soil or might be related to the grass roots and the augmented evapotranspiration.

Identical measurements were carried out on another location which had been used as grassland for at least 35 years. The 2D permittivity distribution measured with the groundwave is shown in Figure 14. Variogram analysis (not shown here) yields an isotropic spatial pattern with a correlation length of 0.35 m.

V. FD CALCULATIONS

In order to determine the influence of soil variability on GPR measurements, FD calculations are carried out. Random media are used which represent the same variability of physical soil properties as in situ. These random media are generated by a sequential Gaussian simulation algorithm [2]. The statistical models which were fitted to the field data are used to determine the input parameters of the simulation. These are, e.g. the mean and variance for a normal distributed physical property as soil permittivity and the correlation length.

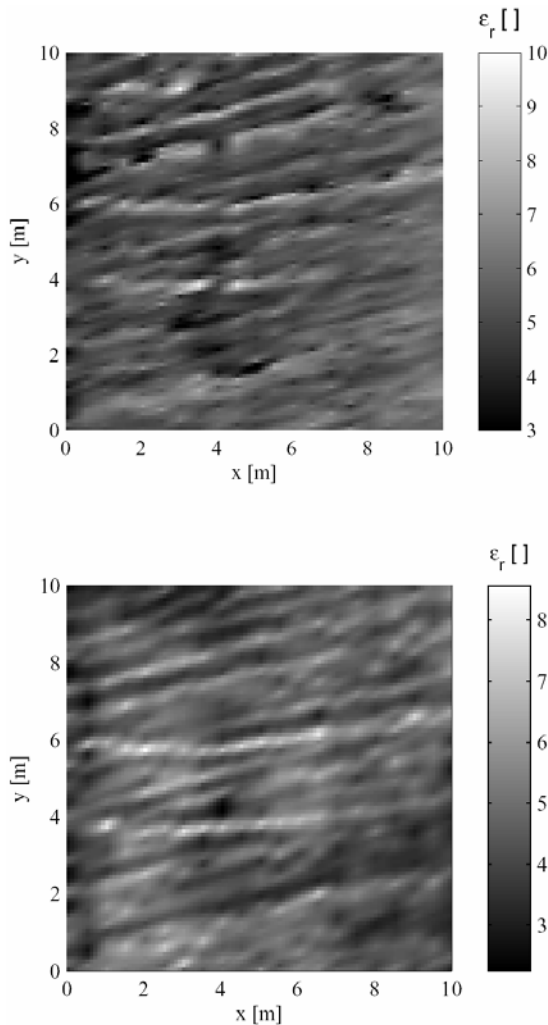


Figure 13. 2D distribution of permittivity on sandy greenland formerly used as an acre derived with the groundwave technique (top) and the coefficient of reflection (bottom). The data are gridded with 0.1 m increment by kriging using an anisotropic variogram model fitted to the directional variograms of Figure 12.

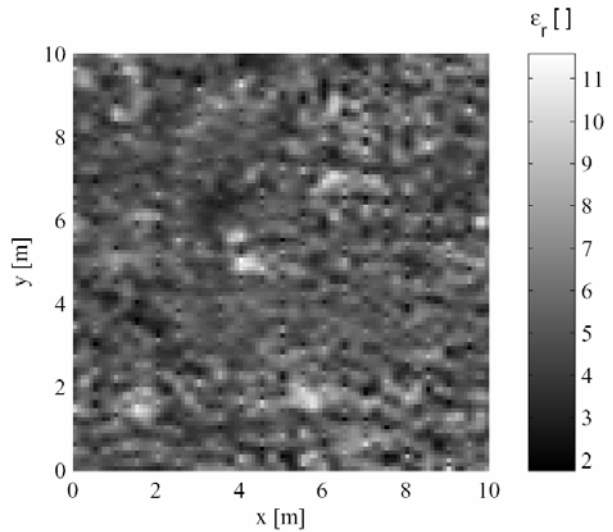


Figure 14. 2D distribution of permittivity on sandy greenland derived with the groundwave. The data are gridded with 0.1 m increment by kriging using an isotropic variogram model.

The influence on GPR measurements is, by way of example, demonstrated for the problem of landmine detection with GPR. Besides metal detectors which are commonly used for landmine detection, GPR is seen to be a useful extension [1]. Due to the short wavelength, GPR can supply an image of small objects like mines in the soil. When metal detectors which base on electromagnetic induction sense only the small metallic detonator inside modern plastic mines, GPR which basis on electromagnetic wave propagation is sensitive to the contrast of permittivity and conductivity of the whole mine relative to the soil. Typical antipersonnel mines are cylindrical objects with approximately 10 cm diameter and 4 cm height. The dielectric properties of modern plastic mines correspond to the permittivity of plastic and explosives which is $\epsilon_r = 3$ with negligible loss tangent [1].

In the models three mines are placed in different soils at a depth of 10 cm. As only principal effects are analysed, the mine model is kept simple and the interior design of the mine as e.g. the plastic housing, explosive body and air gaps is not accounted for. This would need an extremely fine discretisation of the model and might change the backscatter cross section of the mine but not the principle results of the analysis. The physical properties of soils and mines are itemised in Table 1. In model a)–c) permittivity is constant ($\epsilon_r = 5$) and conductivity is spatially variable whereas in model d)–f) permittivity is variable and conductivity is held constant ($\sigma = 0$) (see Figure 15). In model a) conductivity and in model e) permittivity variations are close to the variability determined in field (see above). A FD calculation is performed to simulate a CO measurement with an antenna offset of 10 cm and a centre frequency of 1.5 GHz [10]. Besides a gain function to counterbalance for

geometrical spreading, no further processing was applied to the data to assure a proper comparability of the results (Figure 15).

Table 1. Electromagnetic properties of the soils and mines used for the FD calculations. The mean, standard-deviation (std), coefficient of variation (cv) and the range (a) of the variogram function are listed which are used to generate the heterogeneous models.

model	ε_r []			μ_r []	$\lg(\sigma/(S/m))$		
	mean \pm std	cv	a [m]		mean \pm std	cv	a [m]
a	5	-	-	1	-3 ± 0.15	0.05	0.3
b	5	-	-	1	-2 ± 0.5	0.25	0.3
c	5	-	-	1	-1.5 ± 0.5	0.33	0.3
d	4 ± 0.8	0.2	0.3	1	0	-	-
e	5 ± 1	0.2	0.3	1	0	-	-
f	9 ± 1.8	0.2	0.3	1	0	-	-
mine	3	-	-	1	0	-	-

If soil permittivity is continuous and conductivity is low as is typical for sandy soils, the three mines can clearly be recognised by their diffraction hyperbolas (Figure 15 a). If conductivity is heterogeneous and relatively high, the signals of the three mines are damped differently. The mines can still be detected at mid-range conductivities (Figure 15 b) which are typical for e.g. silty soils. Mine detection will be difficult in the soil of Figure 15 c) as the signal of the left mine is completely damped because it is placed in a high conductive region with $\sigma > 0.1$ S/m. These are typical values for wet salty or some clayey soils.

If soil permittivity is heterogeneous, the form and absolute traveltime of the hyperbolas change due to velocity variations. Another effect of heterogeneity are numberless reflections which interfere with the signals from the mines. The reflections caused by permittivity variations of the models are stronger than the reflections caused even by considerable conductivity variations. If the contrast of the mines to the soil is high as is the case for moist soil with high permittivities, the mine signal is still clearly visible (Figure 15 f). For decreasing water content, the contrast is getting smaller and mines are difficult to detect (Figure 15 e). This model corresponds to permittivity variations which were determined in situ for sandy soils. If water content keeps on decreasing, the mines cannot be detected any more (Figure 15 d).

VI. DISCUSSION

While the geoelectrical method provides information on lateral and vertical variability of conductivity, the two GPR methods provide only information on lateral changes of permittivity. Thus, the variability was investigated only in lateral direction. Vertical anisotropy in the physical properties distribution is not likely to occur in the topsoil as the upper horizon (commonly first 30 cm of the soil) is homogenised due to ploughing, soil freezing and biological activity. The roots of grass, which are mostly restricted to the topsoil, compensate vertical gradients in soil moisture.

Thus, besides anthropogenic anisotropy as e.g. caused by ploughing, an anisotropic distribution of physical properties is, if at all, caused by different soil layers but is not likely to occur in undisturbed topsoils. Therefore, an isotropic distribution was assumed when generating the FD models. If physical properties were distributed anisotropically, they could easily be implemented in geostatistical simulations.

The two GPR methods used to determine permittivity have different sampling depths. The coefficient of reflection is determined by the first few centimetres of the ground [11] so only the very top soil surface is mapped by this method. The depth of influence of the groundwave, i.e. the depth to which the soil is sampled, is controversially discussed in literature [3, 4, 12, 13]. It is a rather complicated function of frequency, antenna separation and permittivity of the ground and still a matter of research. For the antenna frequency used in field of approximately 400 MHz the sampling depth is about one decimetre.

Despite basing on totally different physical background, the two GPR methods yield comparable results in absolute values, variances and spatial pattern of permittivity. The small differences can be explained by different lateral resolution and different sampling depths. The coefficient of reflection yields slightly lower values. This is due to the fact that generally - with the exception directly after precipitation - the absolute values of soil moisture and bulk density are lower at the soil surface.

The analysis of FD simulations shows that, with exception of quite conductive soils ($\sigma > 0.05$ S/m), permittivity fluctuations cause stronger problems in mine detection than conductivity variations. If soil is quite dry and the contrast of the target to the soil is small, heterogeneity in soil moisture and resulting permittivity can cause severe problems to mine detection with GPR.

VII. CONCLUSION AND OUTLOOK

The applied modus operandi including high resolution field measurements, geostatistical analysis, statistical simulation and FD calculation showed to be a powerful tool to determine the influence of geological noise on GPR measurements. The described geophysical techniques yield spatial variability of soil conductivity and permittivity with high spatial resolution. The results of the calculations may be used to assess the uncertainties which might be expected when carrying out measurements under real field conditions. This can help to optimise experimental measuring designs in the run-up of field campaigns or to appraise field data and their interpretation.

There is a lack of non-destructive methods to determine high-resolution soil-permittivity variations with depth. Up to now no non-invasive GPR technique exists which provides permittivity soundings with depth without relying on

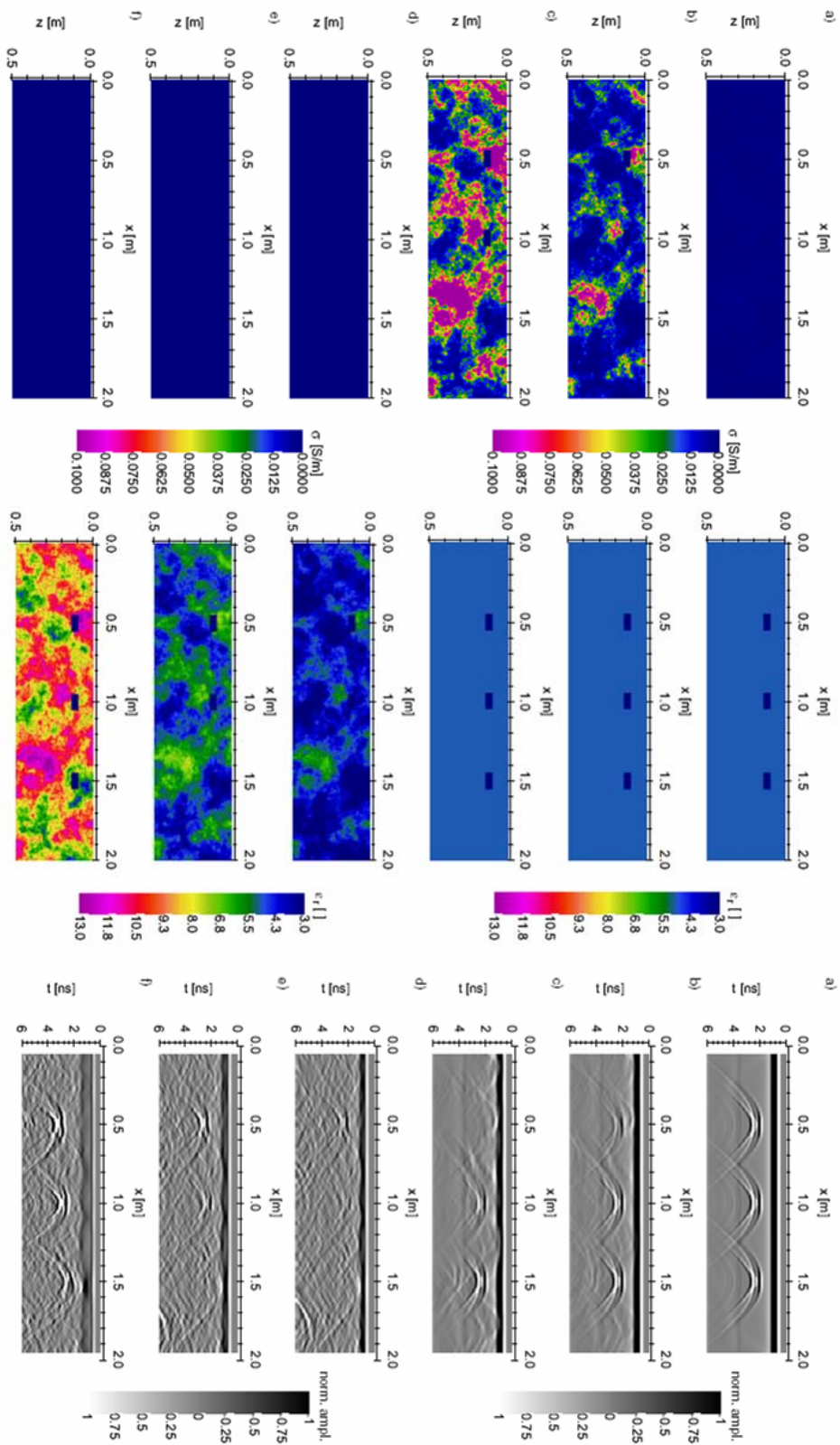


Figure 15. Conductivity (left) and permittivity (centre) distribution of the models and result of CO FD calculation (right).

diffractors or reflectors in the ground. Recent FD calculations have shown that the depth of influence of the proposed 2-receiver groundwave technique depends on the distance between the transmitter and the two receivers. Keeping the distance between both receivers constant and varying the distance between the transmitter and the receivers seems to be a promising technique enabling a vertical permittivity sounding. Combining several of these soundings in combination with an inversion could provide a 2D or 3D permittivity distribution of the ground. However, extensive FD calculations comprising the antennas and measurements under controlled conditions will be needed to understand the complex dependence of the depth of influence from antenna frequency, separation and permittivity distribution of the ground.

So far, conductivity and permittivity have only been determined on sandy soils which are used as grassland. Measurements will be expanded to other soil types and cultivations to obtain typical parameters of spatial pattern of electrical soil properties under other conditions. This information will provide the basis of FD calculations to simulate GPR measurements under various realistic field conditions.

There is a clear link between electrical soil properties and water content so that the presented methods can be used to assess soil moisture. Soil moisture and accordingly electrical properties do not only feature high spatial variability but are also highly variable with time. As the developed techniques are non-destructive, they can repeatedly be applied at the same place. Albeit soil moisture determination with geophysical methods has some limitations concerning accuracy and resolution, the ability of repeated measurements on the same undisturbed soil is a crucial advantage over classical soil scientific methods as e.g. gravimetric soil moisture determination. Repeated measurements will provide important information on how a spatial moisture pattern changes with time, e.g. due to seasonal variations within a hydrologic year, with a unique precipitation event or with cultivation and plant growth. This information will help to understand the formation of hydrophobic and hydrophilic domains, water infiltration and pollution or the interaction of precipitation, soil, vegetation and evapotranspiration. Especially the small-scale heterogeneity of soil moisture is mostly not known and is an important input parameter for weather and climate simulations.

ACKNOWLEDGMENTS

The work was financed by the German Federal Ministry for Education and Research (BMBF) under contract number 01 RX 0310.

REFERENCES

- [1] Bruschini, C., Gros, B., Guerne, F. Pièce, P.-Y. and Carmona, O., "Ground penetrating radar and imaging metal detector for antipersonal mine detection", *Journal of Applied Geophysics*, 40: 59–71 (1998).
- [2] Deutsch, C. V. and Journel, A. G., "GSLIB: Geostatistical Software Library and User's Guide", Oxford University Press (1998).
- [3] Du, S., "Determination of Water Content in the Sub-surface with the Ground Wave of Ground Penetrating Radar", PhD Thesis, Ludwig-Maximilians-Universität München, Germany (1996).
- [4] Galagedara, L. W., Redman, J. D., Parkin, G. W., Annan, A. P. and Endres, A. L., "Numerical modeling of GPR to determine the direct ground wave sampling depth", *Vadose Zone Journal* 4:1096–1106 (2005).
- [5] Günther, T., "Inversion Methods and Resolution Analysis for the 2D/3D Reconstruction of Resistivity Structures from DC Measurements", PhD Thesis, Bergakademie Freiberg, Germany (2004), <<http://www.resistivity.net>>.
- [6] Huisman, J. A., Hubbard, S. S., Redman, J. D. and Annan, A. P., "Measuring soil water content with ground penetrating radar: a review", *Vadose Zone Journal* 2:476–491 (2003a).
- [7] Huisman, J. A., Snepvangers, J. J. J. C., Bouten, W. and Heuvelink, G. B. M., "Monitoring Temporal Development of Spatial Soil Water Content Variation: Comparison of Ground Penetrating Radar and Time Domain Reflectometry", *Vadose Zone Journal* 2:519–529 (2003b).
- [8] Igel, J., "On the Small-Scale Variability of Electrical Soil Properties and Its Influence on Geophysical Measurements", PhD Thesis, Johann Wolfgang Goethe-Universität, Frankfurt a. M., Germany (2007), available at <<http://publikationen.ub.uni-frankfurt.de/volltexte/2007/4785/>>.
- [9] Makinde, W., Favretto-Cristini, N. and de Bazelaire, E., "Numerical modelling of interface scattering of seismic wavefield from a random rough interface in an acoustic medium: comparison between 2D and 3D cases", *Geophysical Prospecting* 53: 373–397 (2005).
- [10] Sandmeier, K. J., "Reflexw-Win, Version 4.2: Windows Program for the Processing of seismic, acoustic or electromagnetic reflection, refraction and transmission data", Sandmeier Software (2006).
- [11] Serbin, G. and Or, D., "Near-surface soil water content measurements using horn antenna radar: methodology and overview", *Vadose Zone Journal* 2:500–510 (2003).
- [12] Sperl, C., "Erfassung der raum-zeitlichen Variation des Bodenwassergehalts in einem Agrarökosystem mit dem Ground-Penetrating Radar", PhD Thesis, TU München, Germany (1999).
- [13] Wollny, K. G., "Die Natur der Bodenwelle des Georadar und ihr Einsatz zur Feuchtebestimmung", PhD Thesis, Ludwig-Maximilians-Universität München, Germany (1999).

12th International Conference on Ground Penetrating Radar, June 16-19, 2008, Birmingham, UK